Elsevier Editorial System(tm) for Optical Materials

Manuscript Draft

Manuscript Number: OM-D-18-00263

Title: Further studies of radiation trapping in Er3+ doped chalcogenide glasses

Article Type: SI: OPTMAT_PRE'17

Keywords: Erbium doping, chalcogenide glass, radiation trapping, photoluminescence.

Corresponding Author: Dr. Cyril Koughia, PhD

Corresponding Author's Institution: University of Saskatchewan

First Author: Cyril Koughia, PhD

Order of Authors: Cyril Koughia, PhD; Chris Craig; Daniel Hewak, Professor

Abstract: Strong overlap of emission and absorption spectra of Er3+ doped glasses gives rise to effect of radiation trapping (RT) where the quanta are emitted, absorbed and re-emitted many times before leaving the volume of the material. We investigate the steady-state and transient PL of Er3+ ions embedded in lanthanum sulphide-oxide glasses with partial substitution of sulfide by oxygen. We develop a technique for direct observation of RT and we show that RT combined with internal reflections leads to uniform spatial distributions of radiation and excited Er3+ ions inside of glass sample.

Highlights (for review)

- Overlap $^4I_{9/2}$-$^4I_{13/2}$ absorption and emission band of Er^{3+} gives rise to radiation trapping,
- A technique to observe radiation trapping in Er^{3+} doped glasses has been developed,
- Radiation trapping + internal reflections lead to uniform distribution inside of doped glass.

*Manuscript
Click here to view linked References

Further studies of radiation trapping in Er^{3+} doped chalcogenide glasses

Cyril Koughia[1], Chris Craig[2], Daniel W. Hewak[2] and Safa Kasap[1]

[1] Department of Electrical and Computer Engineering, University of Saskatchewan, Saskatoon, Canada
[2] Optoelectronics Research Centre, University of Southampton, Southampton, UK SO17 1BJ

Highlights

- Overlap $^4I_{9/2}$-$^4I_{13/2}$ absorption and emission band of Er^{3+} gives rise to radiation trapping,
- A technique to observe radiation trapping in Er^{3+} doped glasses has been developed,
- Radiation trapping + internal reflections lead to uniform distribution inside of doped glass.

Keywords

Erbium doping, chalcogenide glass, radiation trapping, photoluminescence.

Abstract

Strong overlap of emission and absorption spectra of Er^{3+} doped glasses gives rise to effect of radiation trapping (RT) where the quanta are emitted, absorbed and re-emitted many times before leaving the volume of the material. We investigate the steady-state and transient PL of Er^{3+} ions embedded in lanthanum sulphide-oxide glasses with partial substitution of sulfide by oxygen. We develop a technique for direct observation of RT and we show that RT combined with internal reflections leads to uniform spatial distributions of radiation and excited Er^{3+} ions inside of glass sample.

1. INTRODUCTION

Strong overlap of emission and absorption spectra in some molecular or atomic materials gives rise to effect where the quanta are emitted, absorbed and re-emitted many times before leaving the volume of the material. Historically, this effect was first observed in mercury vapors by Lucy J. Hayner during her experiments at Columbia University and reported it 1925 [1]. The text of her paper actually mentions the phrase "radiation imprisonment". Next year, in 1926, in a classical paper entitled “The Diffusion of Imprisoned Radiation Through a Gas”, Edward Arthur Milne was able to describe the observed effect in terms of diffusion [2]. Nowadays, the original term of “radiation imprisonment” is still used in description of mercury discharge (see for example [3]) while “radiation diffusion” is used primarily in plasma physics (for example [4]). Similar effect in solid state physics is usually referred to as “radiation trapping” (RT) or “self-trapping” and it is easily observed in glasses and crystalline hosts doped with trivalent rare earth ions [5 - 13]. In particular, the effect of ”radiation trapping” (RT) is widely investigated in glasses doped with Er^{3+} ions which are known to have strong overlaps for $^4I_{13/2}$–$^4I_{15/2}$ absorption and emission bands [6 - 9,11,14]. Experimentally, the presence of RT is usually demonstrated either by a big difference of PL spectra and/or PL decays in powdered and bulk materials [7,11] or by experiments using excitation and detection trough spatially separated pinholes [15 -17] or by using a confocal setup [18]. It is worth noting here that the effect of radiation trapping may be present also for other overlapping emission/absorption bands such as $^4I_{11/2}$–$^4I_{15/2}$, $^4I_{9/2}$–$^4I_{15/2}$ and others [14].

In the present paper we investigate the effect of RT in lanthanum sulphide-oxide glasses with partial substitution of sulfide by oxygen. We investigate the steady-state and transient PL of Er^{3+} ions embedded in these glasses. We develop a technique for direct observation of RT and we show that RT combined with internal reflections leads to uniform spatial distributions of radiation and excited Er^{3+} ions inside of a cylindrical glass sample.

2. EXPERIMENTAL

The Er^{3+} doped gallium lanthanum sulphide-oxide glasses with two different compositions were prepared at the University of Southampton by melt quenching of raw materials mixed in the following proportions: : 72.5%Ga_2S_3, 27La_2O_3 (high oxide) and 65.8%Ga_2S_3, 31.6%La_2S_3, 2.1%La_2O_3 both samples were doped with 0.5%Er_2S_3. All percent are molar. Melting took place in a vitreous carbon crucible for 24 hours followed by annealing at 500 °C , ramping up and down at 1 °C per minute.

In our research we used three types of samples. (1) *Fine powders* with particle diameters less than 56 μm were prepared by crushing bulk materials and passing them through a sieve with an appropriate mesh. (2) The *plates* with typical thickness around 1 mm were cut off from a glass rod (diameter around 2 mm) and polished on both sides for optical transmittance and PL measurements. (3) *Cylinders* with a variety of lengths were cut off from the same glass rod and polished on both sides. As a result, the cylinders had all shiny surfaces favoring effective imprisonment of light due to internal reflection.

Optical transmittance spectra in the 180 - 3000 nm region were measured using a Perkin Elmer Lambda 900 spectrophotometer on plate samples. The PL spectra were measured using an ORIEL Cornerstone 1/8m monochromator coupled with Oriel InGaAs detector with built-in-amplifier. The PL was excited using laser diodes operating at 808, 980 or 450 nm. If needed, LD beam was modulated by ORIEL mechanical chopper with regulated rotation frequency controlled by an ORIEL chopper controller.

We performed three types of PL measurements. (1) Steady-state PL measurements. (2) Transient PL measurements. In this case the excitation beam was mechanically modulated and the signal from the InGaAs detector built-in-amplifier was directly coupled to PicoScope oscilloscope for registration and further analysis. (3) Quadrature phase PL measurements. Here the signal from the InGaAs detector built-in-amplifier was directly coupled to SR830 DSP lock-in-amplifier while the reference signal with 90° phase shift was supplied by ORIEL chopper controller. This approach was developed and perfected by Prof. Aoki at al. and following his experience we will call this type of experiments QFRS (quadrature frequency resolved spectroscopy) [19 - 24].

3. RESULTS

Figure 1(a)-(e) show the sketches of experimental configurations used in the present paper. The PL of powders were investigated using the setup shown in Figure 1(a). Laser diodes operating at 980, 808 and 450 nm were used as excitation sources. The resulting steady-state PL spectra are shown in Figure 2 (a). The PL decays from steady-state values (shown in Figure 2 (b)) were measured by mechanically interrupting the laser beam. In some experiments the powders were submerged in glycol. It is worth noting that PL spectra and PL decay rates seem to be not effected by the excitation wavelength and surrounding media.

Bulk samples (in the shape of cylinders shown in Figure 1(f)) were investigated using the setup shown in Figure 1(b). Here we used primarily weekly absorbed 808 and 980 nm PL excitation to achieve uniform excitation throughout the volume of the sample. The results of

measurements are presented in Figure 3 and reveal the strong influence of sample size on PL spectra and PL decay times for both $^4I_{13/2}$-$^4I_{15/2}$ and $^4I_{11/2}$-$^4I_{15/2}$ Er^{3+} emission bands. In particular, Figure 3 (c) and (d) show that PL decay becomes slower in larger samples (longer cylinders).

Figure 4 compares PL spectra and PL decays measured in powder and a 10 mm long cylinder (similar to that shown in Figure 1(f)) in air and glycol (see setup in Figure 1(c)). It is clearly seen that the submersion in glycol makes PL spectrum narrower and the PL decays faster (but not as narrow and fast as in powder).

Figure 5(a) compares the PL decay measured using the setup shown in Figure 1(d) with PL decay in powder (measured using the setup Figure 1(a)) and in bulk (cylindrical) samples (setup Figure 1(b)). PL decays in powder (PL_p) and in bulk (PL_b) samples seem to be exponential with decay times τ_p and τ_b, respectively. Meanwhile, the PL decay using the setup of Figure 1(d) may be approximated by a sum of two exponentials having the same characteristic times τ_p and τ_b.

Figure 5(b) compares QFRS PL spectra measured for powder (see Figure 1 (a)) and bulk sample (26 mm cylinder) measured as in Figure 1 (b). One can notice a shift of the powder spectrum towards higher frequencies, correlating with smaller decay times in accordance with previous results shown in Figure 3(c).

The experiment shown in Figure 1 (d) produces a combination of PL_p and PL_b and Figure 6(a-c) shows the results of these experiments where the PL_p/PL_b ratio has been varied by submersion of the bulk sample into glycol (Figure 6(a)), or by means of QFRS (Figure 6(b)), or by the combination of both methods (Figure 6(c)). Figure 6(d)-(f) shows the difference appearing in collected spectra due to submersion into glycol or/and variations of excitation frequency (in QFRS), which may be associated with PL_b as it is discussed in the next section.

Finally, Figure 7(a) shows the result of averaging spectra from Figure 6(a)-(c) and Figure 7(b) makes a comparison with the results of PL measurements in bulk samples which has been presented earlier in Figure 3(a) as curve 4.

4. DISCUSSION

Before discussing RT, we need to rule out another reason of PL spectra broadening in heavily Er^{3+} doped glasses, which is clustering of ions [25]. This may be achieved by performing the experiments on fine powders. Figure 2 shows PL spectra and PL decays measured on fine powders of Er^{3+} doped glass. One can see the clear independence of results against changes in the excitation wavelength or surrounding media. Further, the PL spectrum closely follows the prediction of McCumber theory [26] developed for isolated ions and connecting absorption ($\sigma_a(\nu)$) and emission cross-sections ($\sigma_e(\nu)$)

$$\sigma_e(\nu) = \sigma_a(\nu)\exp\left(\frac{h\varepsilon - h\nu}{k_B T}\right) \tag{1}$$

where $h\nu$ is the energy of the emitted or absorbed photon, and $h\varepsilon$ is the net thermodynamic free energy required to move one Er^{3+} ion from the ground ($^4I_{15/2}$) state to the excited ($^4I_{13/2}$) state. The main assumption for Equation (1) states that "the time required to establish a thermal distribution within each manifold is short compared with the lifetime of this manifold" [27]. Additionally, all measured PL decays seem to follow exponential dependences with the same characteristic time equal to τ_D = 3.27 ms which is close to τ_{JO}=3.33 ms derived using Judd-Ofelt analysis [28, 29]. All above results suggest the absence of clusters. Therefore, PL spectra deformation as well as PL decay time variation (clearly seen in Figure 3 for both $^4I_{13/2}$-$^4I_{15/2}$ and $^4I_{11/2}$-$^4I_{15/2}$ bands) should be attributed to RT.

So far it seems obvious that RT is directly connected to the sample size. But more precisely one should use the "effective" size of the sample. The word "effective" implies the effect of internal reflections which may substantially increase the optical path of radiation inside of the sample making it optically "bigger". Gallium lanthanum sulphide glasses used in present research exhibit large refractive indices in excess of 2.36 [30] which may lead to effective internal reflections particularly important for samples in the shape of polished cylinders (Figure 1(f)). Figure 4 clearly supports these considerations. The submersion of the sample into glycol obviously reduces the amount of internal reflections, which leads to acceleration of PL decay and the narrowing of PL spectrum. As a result, we can conclude that RT is stimulated by the presence of internal reflection and is intertwined with this effect.

Now, let us show that the distribution of radiation and excited ions inside the sample produced by RT is uniform. Figure 5 shows the results of experiments sketched in Figure 1(d). In this experiment, the excitation at 808 nm pumps the powder whose emission corresponding to $^4I_{13/2}$-$^4I_{15/2}$ band passes through long-pass filter and serves as excitation for the $^4I_{13/2}$-$^4I_{15/2}$ PL in a bulk (cylinder) sample. Therefore, in this experiment, the PL of the bulk (PL_b) is directly related to the share of radiation of powder trapped in the bulk. We will characterize PL_b, firstly, by decay time and, secondly, by spectrum. It seems obvious that the emission collected in setup Figure 1(d) is the mixture of RT related PL of the bulk (PL_b) and a share of emission of powder that has avoided absorption while passing the bulk sample (PL_p). Figure 5 seems to support this intuitive conclusion. It shows that the decay of PL collected in setup of Figure 1(d) may be presented as a combination of two exponentials with characteristic times τ_p and τ_b which are typical for powder and uniformly excited bulk material measured in experiments in Figure 1(a) and (b), respectively. The faster exponential in this experiment may be associated with PL_p and the slower one with PL_b. This is the first conclusion. PL_b, which is directly related to radiation trapped in bulk material, shows the same decay time as that from a uniformly excited bulk sample. The next step involves uncovering the spectrum of PL_b by separating the mix of PL_p and PL_b collected together in the experiments from Figure 1(d). For example, we know that PL_b is slower than PL_p (Figure 5(a)). Therefore, PL_p and PL_b may be separated by using the QFRS technique, the theory and practice of which are discussed in detail in many references [19,20,21,22,23,24]. Figure 5(b) shows QFRS for powdered (PL_p) and bulk (PL_b) samples. As it is expected, the signal for bulk material is slightly shifted toward lower modulation frequencies. Therefore, the spectral scan of mixture ($PL_b + PL_p$) collected at 4.5Hz (Φ_3) would contain higher contribution from the bulk material than the scan measured at 30 Hz (Φ_4). The comparison of these two spectra (Φ_3 and Φ_4) is done in Figure 6(b) and their difference ($\Delta\Phi_{34} = \Phi_3 - \Phi_4$), which may be attributed to PL_b, is shown in Figure 6(e).

Another way to uncover the spectrum of PL_b is to immerse the sample into a liquid (glycol) as shown in Figure 1(e). It seems intuitively clear that the propagation of PL_p and PL_b inside the bulk sample will be different and will be differently affected by submersion into glycol due to the distortion introduced by internal reflections. The resulting spectra (Φ_1 and Φ_2) are shown in Figure 6(a) and their difference ($\Delta\Phi_{12} = \Phi_1 - \Phi_2$), which again may be attributed to PL_b is shown in Figure 6(d). Finally, Figure 6(c) illustrates the mixture of two approaches (submersion into glycol combined with QFRS gives spectrum Φ_5) and the difference of spectra ($\Delta\Phi_{15} = \Phi_1 - \Phi_5$) is shown in Figure 6(f). The differential spectra in Figure 6(d(-(f) are quite noisy but the presentation quality is improved by averaging, which is shown in Figure 7(a).

Finally, Figure 7(b) compares the averaged spectrum ($\Delta\Phi$) associated with PL_b with the spectrum of PL collected in the same bulk sample under uniform excitation in the experiment sketched in Figure 1(b) (see curve 4 in Figure 3(a)). Both spectra turn out to be surprisingly

similar. Therefore, we can conclude that radiation trapping related PL (PL_b) and PL obtained by uniform excitation of the same bulk sample have similar spectra and temporal characteristics which assume that they are generated by similar spatial distributions of excited ions and radiation. We conclude that these distributions are just uniform..

5. CONCLUSIONS

We have investigated the steady-state and transient PL of Er^{3+} ions embedded in lanthanum sulphide-oxide glasses with compositions ($65.8\%Ga_2S_3+31.6\%La_2S_3+2.1\%La_2O_3+0.5\%Er_2S_3$) and ($72.5\%Ga_2S_3+ 27La_2O_3+0.5\%Er_2O_3$). The photoluminescence spectrum and photoluminescence decay corresponding to the $^4I_{13/2}$-$^4I_{15/2}$ emission band in fine powders closely follows the theoretical predictions for isolated ions, ruling out possible Er^{3+} clusterization. The PL decay lifetime is very close to that reported in Judd-Ofelt analysis. The increase of geometrical size of samples leads to significant broadening of the photoluminescence spectra and decay deceleration corresponding to the $^4I_{13/2}$-$^4I_{15/2}$ and $^4I_{11/2}$-$^4I_{15/2}$ emission bands. These effects are explained by the presence of radiation trapping, understood as a chain of consecutive emission-absorption events. We demonstrated direct observation of radiation trapping by exciting bulk samples with the same band emission emanating from powders. We have shown that radiation trapping stimulated by internal reflections, achieved by immersing the Er^{3+}-doped glass rods in glycol, leads to a uniform distribution of radiation and excited Er^{3+} ions inside of glass rod sample.

Acknowledgments

We thank Jordan Wong for participating in some of the optical measurements. Southampton acknowledged the support of the Engineering and Physical Sciences Research Council, United Kingdom, through grant EP/M015130/1, Manufacturing and Application of Next Generation Chalcogenides. The University of Saskatchewan acknowledges financial support NSERC.

Figures (TIFF, JPEG, PDF)

Figure 1. Configurations of PL experiments used in the present paper. Abbreviations PL_p and PL_b stand for PL emanating from powder or bulk material, respectively. (a) Measurement of PL of powdered materials. (b) Measurement of PL of bulk glass shaped as a cylinder (rod) (see (f)). (c) Experiment is similar to (b) but the glass cylinder is immersed in glycol. (d) PL of powder passes through long pass filter and acts as excitation for PL in the bulk sample. The resulting PL contains both PL_p and PL_b. (e) Experiment is similar to (d) but the central part of bulk sample is immersed in glycol which effectively reduces PL_b (see the text for explanations). (f) Picture of two typical glass cylinders used in present experiments. Glass compositions are
($72.5\%Ga_2S_3+27La_2O_3+0.5\%Er_2O_3$) (upper cylinder) and
($65.8\%Ga_2S_3+31.6\%La_2S_3+2.1\%La_2O_3+0.5\%Er_2S_3$) (lower cylinder).

Figure 2. PL spectra in comparison with McCumber theory [26] (a) and PL decays (b) corresponding to $^4I_{13/2}$-$^4I_{15/2}$ transitions in Er^{3+} ions in powders of ($65.8\%Ga_2S_3+31.6\%La_2S_3+2.1\%La_2O_3+0.5\%Er_2S_3$) glass. Powder particle diameter <56 μm. Measurement method is illustrated in Figure 1(a). Excitation wavelengths and media used in measurements are specified in legends.

Figure 3. PL spectra (a, b) and PL decays (c, d) corresponding to $^4I_{13/2}$-$^4I_{15/2}$ (a, c) and $^4I_{11/2}$-$^4I_{15/2}$ (c, d) transitions in different samples of ($65.8\%Ga_2S_3+31.6\%La_2S_3+2.1\%La_2O_3+0.5\%Er_2S_3$) glass. Curves (1) are measured in powders with experimental setup shown in Figure 1(a). Curves (2) are collected for plates with thickness 1 mm. Curves (3) and (4) are for cylinders with diameters 2 mm and lengths 10 and 26 mm, respectively. Experimental setup is shown in Figure 1(b). For all samples, the excitation wavelength has been 808 nm corresponding to $^4I_{15/2}$-$^4I_{9/2}$ transition. Straight black lines in (c) and (d) represent exponential approximations aimed to estimate PL decay times.

Figure 4. PL spectra (a) and PL decays (b) corresponding to $^4I_{13/2}$-$^4I_{15/2}$ Er^{3+} transitions in ($65.8\%Ga_2S_3+31.6\%La_2S_3+2.1\%La_2O_3+0.5\%Er_2S_3$) glass. Curves (1) are measured in powders with experimental setup shown in Figure 1(a). Curves (2) and (3) are collected for a cylinder with length 10 mm and diameter 2 mm. Curves (2) are measured in air (Figure 1(b)). Curves (3) are measured in glycol (Figure 1(c)). For all samples, the excitation wavelength has been 808 nm corresponding to $^4I_{15/2}$-$^4I_{9/2}$ transition. Straight black lines in (b) represent exponential approximations used to estimate PL decay times.

Figure 5. (a) Comparison of PL decays measured in experiments sketched in Figure 1 (a), (b) and (d). PL_p is the PL of powder measured as in Figure 1 (a) and its decay may be approximated by $\exp(-t/\tau_p)$. Similarly, PL_p is the PL of bulk material measured as in Figure 1 (b) with decay following $\exp(-t/\tau_b)$. The experiment sketched in Figure 1 (d) produces a combination of PL_p and PL_b which may be approximated by a linear combination of the two above exponentials. Black lines (solid and broken) are exponentials $\exp(-t/\tau_p)$ and $\exp(-t/\tau_b)$ as well as their linear combinations. Glass ($65.8\%Ga_2S_3+31.6\%La_2S_3+2.1\%La_2O_3+0.5\%Er_2S_3$).

(b) QFRS spectra measured for powder as in Figure 1 (a) and bulk sample (26 mm cylinder) measured as in Figure 1 (b). In both cases, the excitation is at 808 nm. Broken lines are guides to eye corresponding to 4.5 and 30 Hz. Same glass as in Figure 5(a).

Figure 6. (a) Comparison of PL spectrum Φ_1 measured in air (as in Figure 1(d)) with PL spectrum Φ_1 measured for the sample immersed in glycol (see Figure 1(e)). (b) Comparison of QFRS spectrum Φ_3 measured at 4.5 Hz with QFRS spectrum Φ_4 measured at 30 Hz. Both Φ_3 and Φ_4 have been measured in air (Figure 1(d)). (c) Comparison of QPPL spectrum Φ_5 measured at 30 Hz in glycol (Figure 1(e)) with Φ_1 introduced earlier. (d)-(e) Differential spectra $\Delta\Phi_{12} = \Phi_1 - \Phi_2$, $\Delta\Phi_{34} = \Phi_3 - \Phi_4$ and $\Delta\Phi_{15}=\Phi_1 - \Phi_5$, respectively. Bulk sample has a shape of cylinder with diameter 2 mm and length 26 mm. Glass composition is ($65.8\%Ga_2S_3+31.6\%La_2S_3+2.1\%La_2O_3+0.5\%Er_2S_3$).

Figure 7. (a) Averaging of differential spectra $\Delta\Phi_{12}$, $\Delta\Phi_{34}$ and $\Delta\Phi_{15}$ presented in Figure 6 (d)-(e), respectively. The averaged spectrum $\Delta\Phi$ is shown by thick solid blue line. (b) Comparison of $\Delta\Phi$ with the PL spectrum of the same bulk sample measured as in Figure 1(b) using weakly absorbed excitation at 980 nm (Φ_6). Glass composition and sample geometry are the same as in Figure 6.

REFERENCES

[1] Lucy J. Hayner, The persistence of the radiation excited in mercury vapor, Phys. Rev 26 (1925) 364-375; https://doi.org/10.1103/PhysRev.26.364

[2] E. A. Milne, The diffusion of imprisoned radiation through a gas, J. London Math. Soc., S1 (1926) 40-51. doi: 10.1112/jlms/s1-1.1.40

[3] J.B. Anderson, Monte Carlo treatment of resonance-radiation imprisonment in fluorescent lamps—revisited, J. Phys. D. Appl. Phys. 49 (2016) 495501. http://stacks.iop.org/0022-3727/49/i=49/a=495501.

[4] C. C. Smith, Solutions of the radiation diffusion equation, High Energy Density Physics, 6 (2010) 48. doi.org/10.1016/j.hedp.2009.06.009

[5] F. Auzel, F. Bonfigli, S. Gagliari, G. Baldacchini, The interplay of self-trapping and self-quenching for resonant transitions in solids; Role of a cavity, J. Lumin. 94–95 (2001) 293–297. doi:10.1016/S0022-2313(01)00308-8.

[6] F. Auzel, G. Baldacchini, L. Laversenne, G. Boulon, Radiation trapping and self-quenching analysis in Yb^{3+}, Er^{3+}, and Ho^{3+} doped Y_2O_3, Opt. Mater. (Amst). 24 (2003) 103–109. doi:10.1016/S0925-3467(03)00112-5.

[7] C. Koughia, S.O. Kasap, Excitation diffusion in GeGaSe and GeGaS glasses heavily doped with Er^{3+}, Opt. Express. 16 (2008) 7709–7714. doi:10.1364/OE.16.007709.

[8] C. Koughia, C. Craig, D.W. Hewak, S. Kasap, Tailoring the $^4I_{9/2} \rightarrow {}^4I_{13/2}$ emission in Er^{3+} ions in different hosts media, Opt. Mater. (Amst). 41 (2015) 116–121. doi:10.1016/j.optmat.2014.09.013.

[9] J. A. Muñoz, G. Herreros, F. Lifante, Cussó. Concentration dependence of the 1.5 mm emission lifetime of Er^{3+} in $LiNbO_3$ by radiation trapping, Phys.Stat.Sol.(a), 168 (1998) 525.

[10] D.S. Sumida, T. Y. Fan, Effects of radiation trapping on fluorescence lifetime and emission cross section measurements in solid-state laser media", Optics Letters, 19 (1994) 1343-1345.

[11] M. Mattarelli, M. Montagna, L. Zampedri, A. Chiasera, M. Ferrari, G. C. Righini, L. M. Fortes, M. C. Gonçalves, L. F. Santos, R. M. Almeida, Self-absorption and radiation trapping in Er^{3+}-doped TeO_2-based glasses, EPL (Europhysics Lett. 71 (2005) 394. http://stacks.iop.org/0295-5075/71/i=3/a=394.

[12] V. G. Babajanyan, R. B. Kostanyan, P. H. Muzhikyan, Spectral and kinetic peculiarities of the radiation trapping effect in doped materials, Opt. Mater., 45 (2015) 215.

[13] C.-H. Chen, Y.-H. Wu, C.-P. Fan, T.-H. Wei, Saturation of radiation trapping and lifetime measurements in three-level laser crystals, Opt. Express. 20 (2012) 25613. doi:10.1364/OE.20.025613.

[14] S. Kasap, C. Koughia, The influence of radiation trapping on spectra and measured lifetimes of $^4F_{9/2}$ -$^4I_{15/2}$, $^4I_{9/2}$ -$^4I_{15/2}$, $^4I_{11/2}$ -$^4I_{15/2}$ and $^4I_{13/2}$ -$^4I_{15/2}$ emission bands in GeGaS glasses doped with erbium, Int. Conf. Transparent Opt. Networks. 2016–Augus (2016) 13–17. doi:10.1109/ICTON.2016.7550252.

[15] H. Kühn, S. T. Fredrich-Thornton, C. Kränkel, R. Peters, K. Petermann, Model for the calculation of radiation trapping and description of the pinhole method, Optics Letters, 32 (2007) 1908.

[16] G. Toci, Lifetime measurements with the pinhole method in presence of radiation trapping, Appl. Phys. B, 106 (2012) 63.

[17] G. Toci, D. Alderighi, A. Pirri, M. Vannini, Lifetime measurements with the pinhole method in presence of radiation trapping: II - Application to Yb^{3+} doped ceramics and crystals, Appl. Phys. B Lasers Opt. 106 (2012) 73–79. doi:10.1007/s00340-011-4632-y.

[18] Y.-S. Ong, S. Aravazhi, S . A. Vázquez- Córdova, J. J. Carvajal, F. Díaz, J. L. Herek, S. M. García-Blanco, M. Pollnau, Direct confocal lifetime measurements on rare-earth-doped media exhibiting radiation trapping, Optical Materials Express, 7 (2017) 527–532. doi:10.1364/OME.7.000527.

[19] K. Koughia, D. Saitou, T. Aoki, M. Munzar, S.O. Kasap, Photoluminescence lifetime spectrum in erbium doped Ge-Ga-S glasses, J. Non. Cryst. Solids. 352 (2006) 2420–2424. doi:10.1016/j.jnoncrysol.2006.03.019.

[20] S.O. Kasap, K. Koughia, M. Munzar, D. Tonchev, D. Saitou, T. Aoki, Recent photoluminescence research on chalcogenide glasses for photonics applications, J. Non. Cryst. Solids. 353 (2007) 1364–1371. doi:10.1016/j.jnoncrysol.2006.10.060.

[21] K. Koughia, M. Munzar, T. Aoki, S.O. Kasap, Photoluminescence spectra and lifetimes of $^4I_{13/2}$ -$^4I_{15/2}$ and $^4I_{11/2}$ -$^4I_{15/2}$transitions in erbium doped GeGaSe and GeGaS glasses, J. Mater. Sci. Mater. Electron. 18 (2007) 153–157. doi:10.1007/s10854-007-9189-5.

[22] T. Aoki, D. Saitou, K. Fujimoto, C. Fujihashi, K. Shimakawa, K. Koughia, S.O. Kasap, Quadrature frequency resolved spectroscopy (QFRS) of radiative transitions of Er^{3+} and Nd^{3+} ions in chalcogenide glasses (ChGs), J. Phys. Conf. Ser. 253 (2010). doi:10.1088/1742-6596/253/1/012010.

[23] L. Strizik, V. Prokop, J. Hrabovsky, T. Wagner, T. Aoki, Quadrature frequency resolved spectroscopy of upconversion photoluminescence in GeGaS:Er^{3+}: I. Determination of energy transfer upconversion parameter, J. Mater. Sci. Mater. Electron. 28 (2017) 7053–7063. doi:10.1007/s10854-016-6306-3.

[24] T. Aoki, L. Strizik, J. Hrabovsky, T. Wagner, Quadrature frequency resolved spectroscopy of upconversion photoluminescence in GeGaS:Er^{3+}; II. Elucidating excitation mechanisms of red emission besides green emission, J. Mater. Sci. Mater. Electron. 28 (2017) 7077–7082. doi:10.1007/s10854-017-6363-2.

[25] R. El-Mallawany, A. Patra, C.S. Friend, R. Kapoor, P.N. Prasad, Study of luminescence properties of Er^{3+}-ions in new tellurite glasses, Opt. Mater. (Amst). 26 (2004) 267–270. doi:10.1016/j.optmat.2004.01.002.

[26] D.E. McCumber, Einstein Relations Connecting Broadband Emission and Absorption Spectra, Phys. Review, 136 (164) A954.

[27] R.S. Quimby, W.J. Miniscalco, B. Thompson, Clustering in erbium-doped silica glass fibers analyzed using 980 nm excited-state absorption, J. Appl. Phys. 76 (1994) 4472–4478. doi:10.1063/1.357278.

[28] B.R. Judd, Optical Absorption Intensities of Rare-Earth Ions, Phys. Rev. 127 (1962) 750–761. https://link.aps.org/doi/10.1103/PhysRev.127.750.

[29] G.S. Ofelt, Intensities of Crystal Spectra of Rare-Earth Ions, J. Chem. Phys. 37 (1962) 511–520. doi:10.1063/1.1701366.

[30] C.C. Ye, D.W. Hewak, M. Hempstead, B.N. Samson, D.N. Payne, Spectral properties of Er^{3+}-doped gallium lanthanum sulphide glass, J. Non. Cryst. Solids. 208 (1996) 56–63. doi:10.1016/S0022-3093(96)00203-7.

Figure

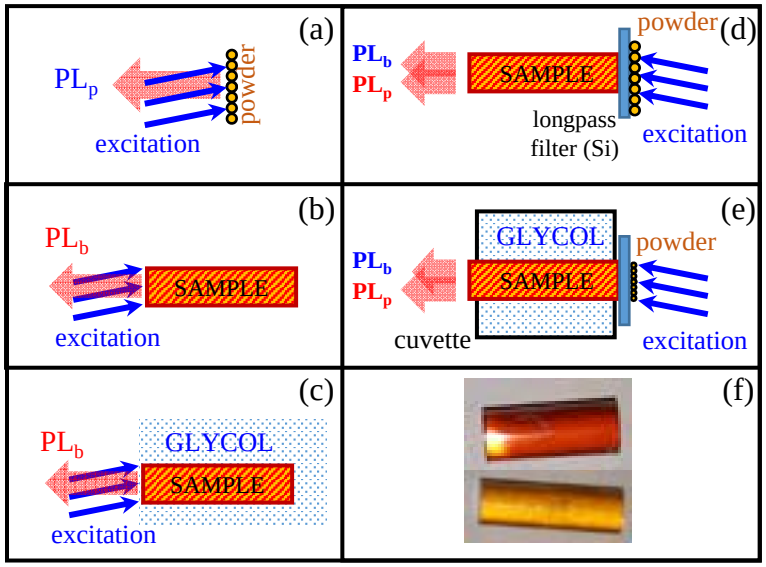
(a)
PL_p
powder
excitation
(b)
PL_b
SAMPLE
excitation
(c)
PL_b
GLYCOL
SAMPLE
excitation
(d)
powder
PL_b
PL_p
SAMPLE
longpass
filter (Si)
excitation
(e)
GLYCOL
powder
PL_b
PL_p
SAMPLE
cuvette
excitation
(f)

Figure
Click here to download high resolution image

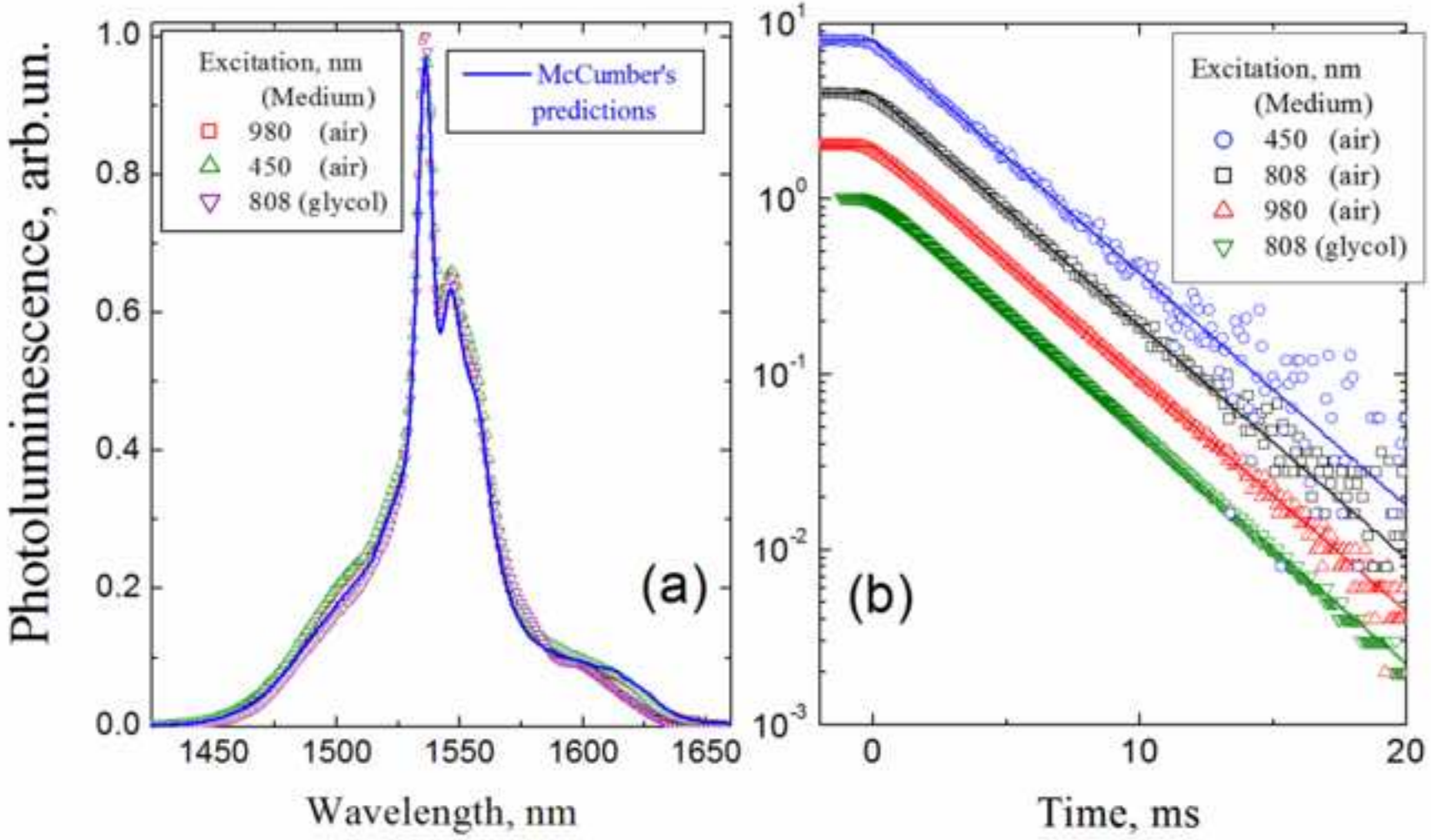

Figure
Click here to download high resolution image

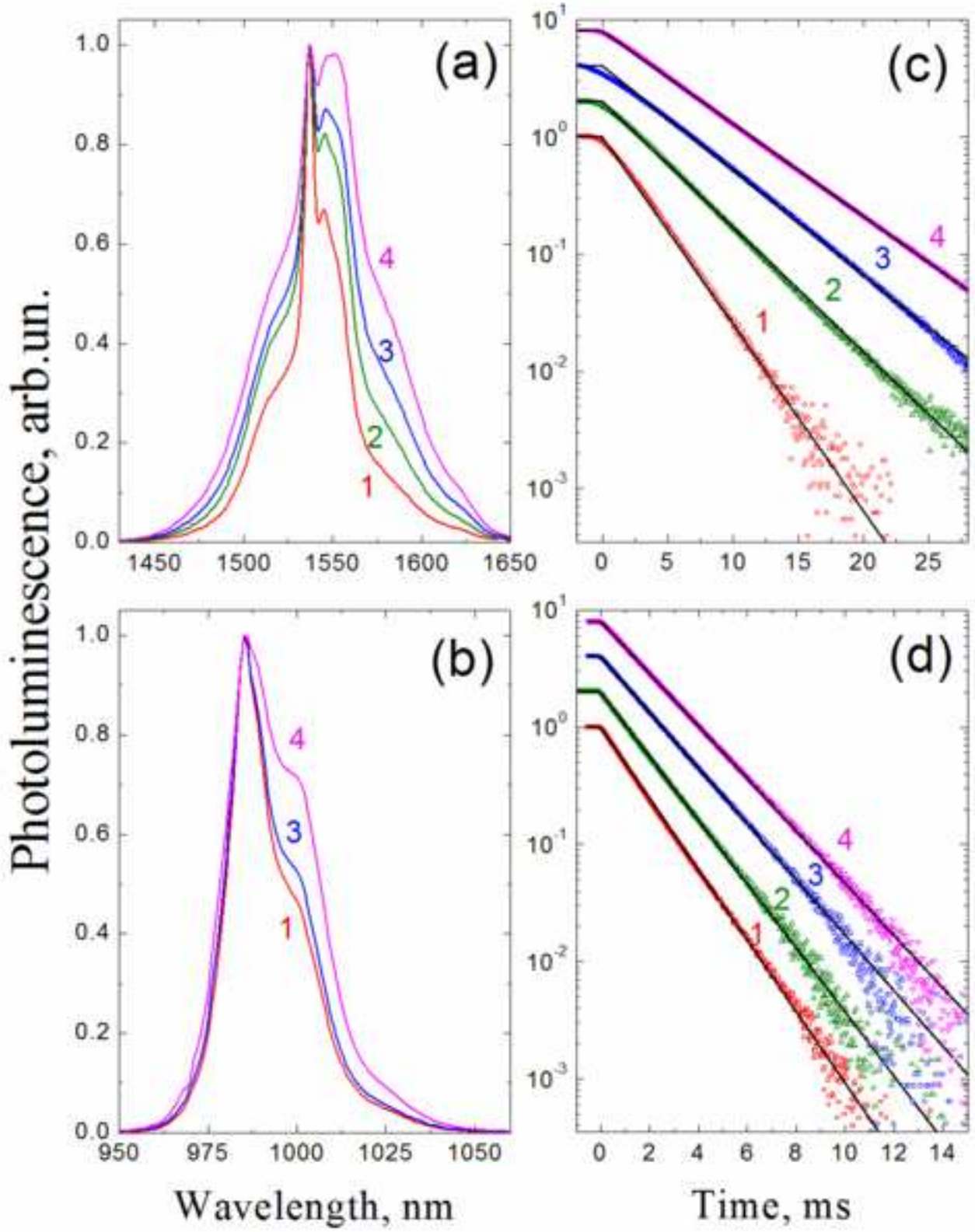

Figure
Click here to download high resolution image

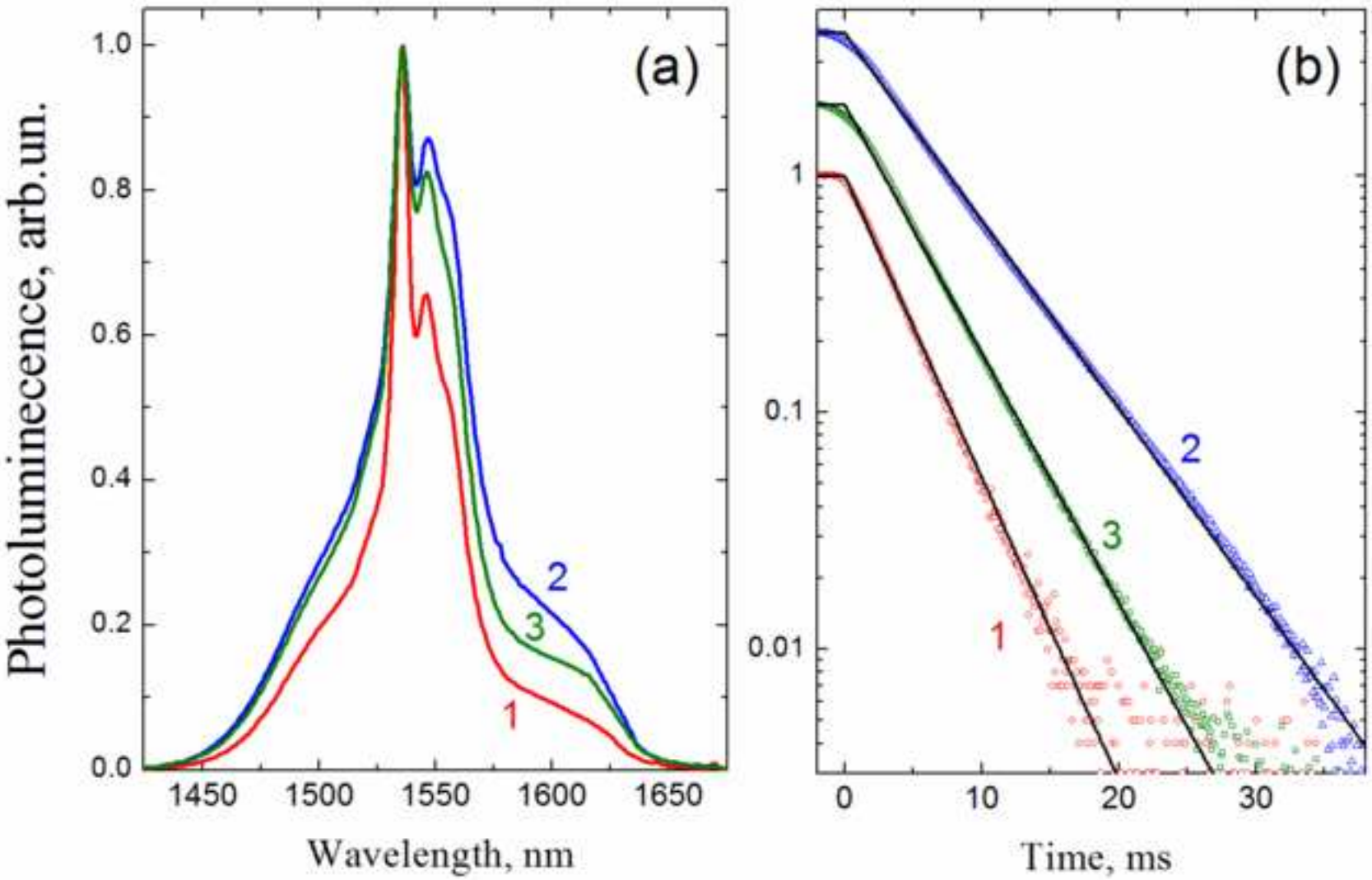

Figure
Click here to download high resolution image

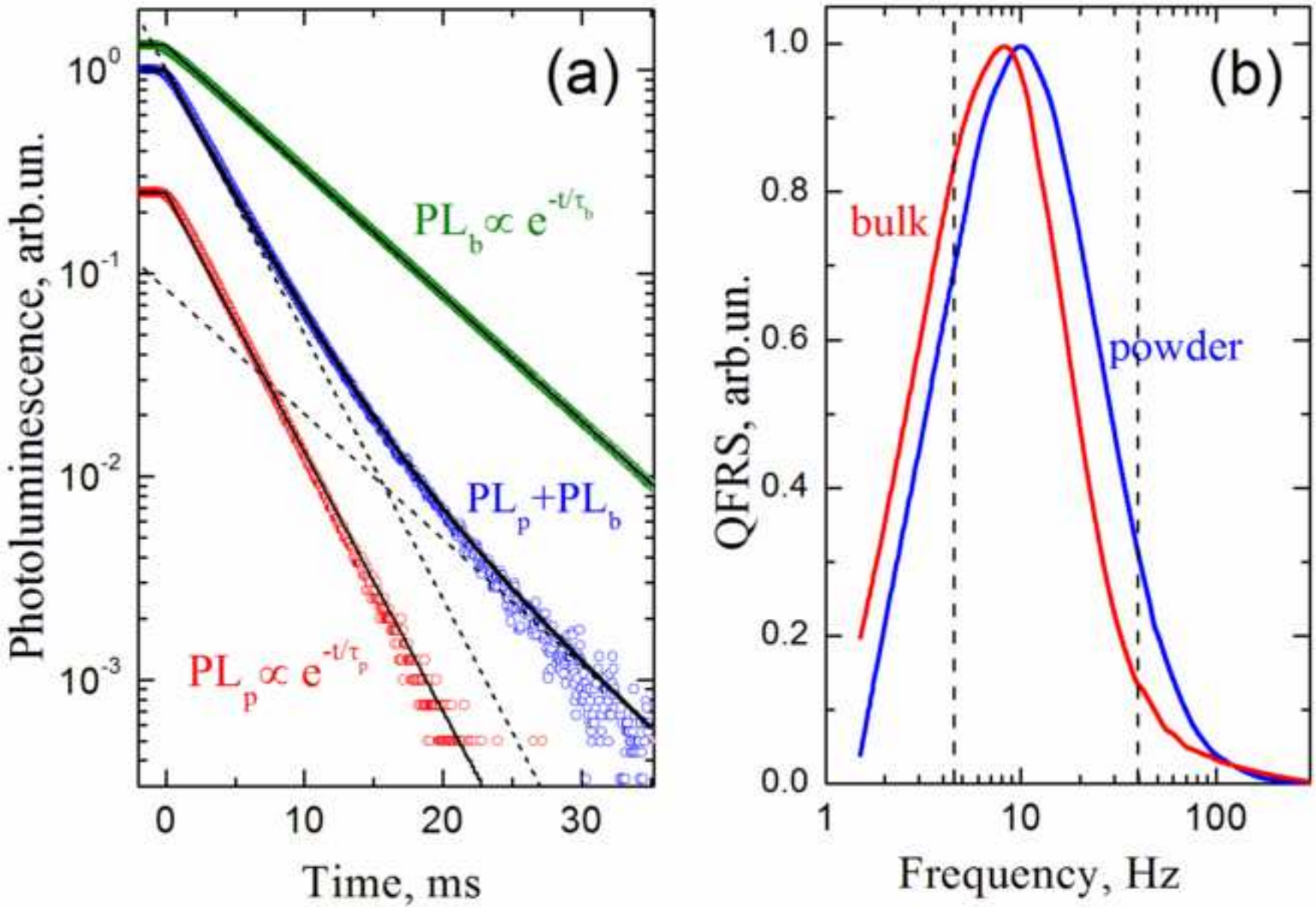

Figure

Click here to download high resolution image

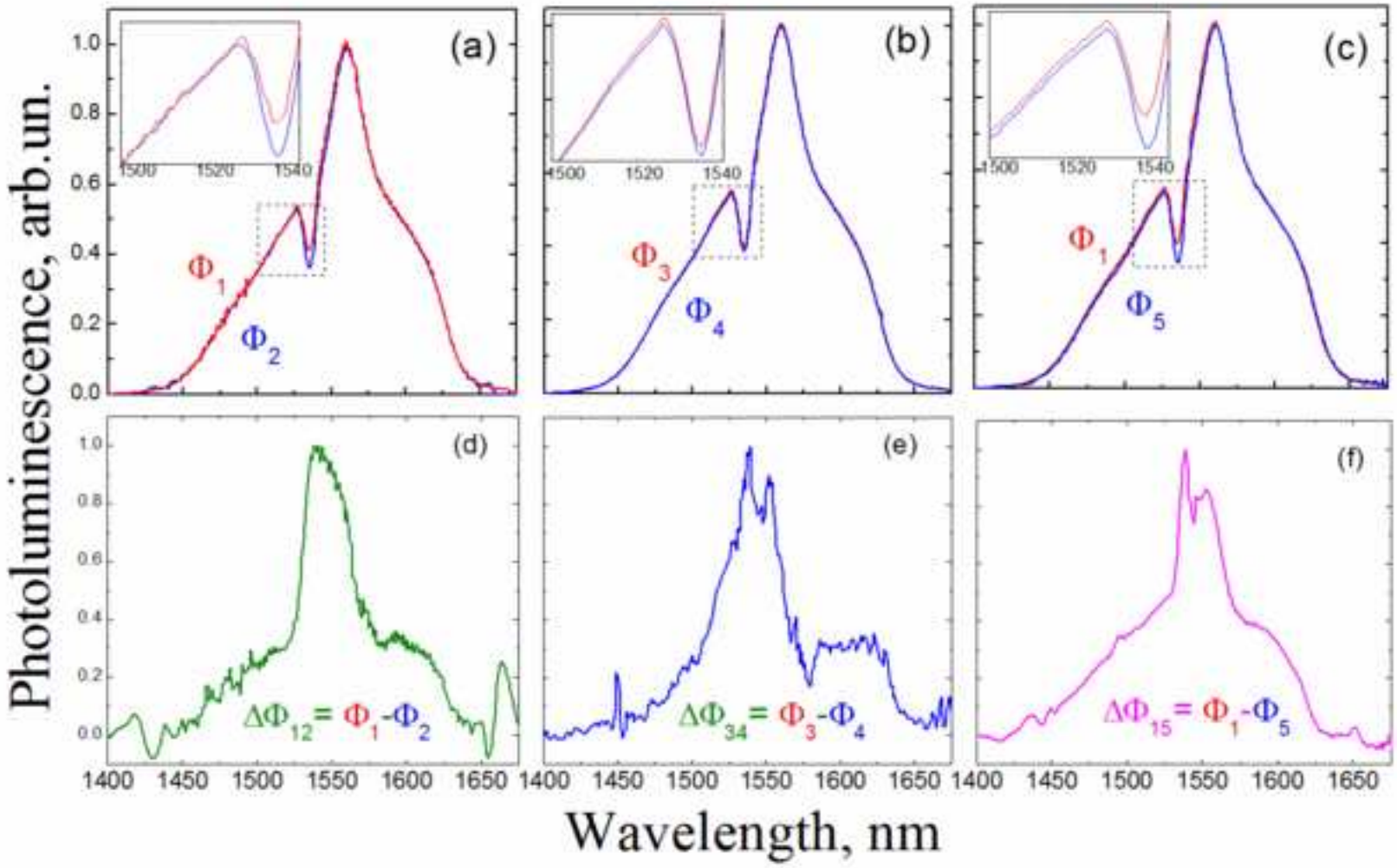

Figure

Click here to download high resolution image